

Suppression of leakage for a charge quadrupole qubit in triangular geometry

Guo Xuan Chan¹ and Xin Wang^{1,*}

¹*Department of Physics, City University of Hong Kong,
Tat Chee Avenue, Kowloon, Hong Kong SAR, China,
and City University of Hong Kong Shenzhen Research Institute, Shenzhen, Guangdong 518057, China*
(Dated: January 15, 2019)

We present a simple yet effective strategy to suppress the leakage in the charge quadrupole qubit system by having the dots in a triangle as opposed to the linear geometry originally conceived. We find that the tunnel coupling between the two outmost dots are amplified in triangular triple dots, which consequently reduces leakage by separating the leaked state and qubit states. We have found that the leakage can be suppressed by as much as five orders of magnitude when the dots form an equilateral triangle, with further improvement of control fidelities possible if composite pulses are applied.

Introduction. Semiconductor quantum dots are promising candidates to realize quantum computing. In the simplest proposal of a double-quantum-dot charge qubit, an electron can occupy either one dot or the other, serving as the two logical states [1]. Universal single-qubit operations of the charge qubit can be achieved by alternating the relative energy between the two dots [2, 3], and two-qubit gates can be performed using the electrostatic coupling between them [4–6]. While this charge qubit can have very fast gate operations, it at the same time suffers heavily from charge noises, leading to very short coherence times [7–12]. Various proposals have been put forward to improve the control of charge qubits for quantum information processing, including ultrafast gates [13], ac control around certain sweet spots [14], or hybrid qubits that combine advantages of manipulating charge and spin states [15–19].

Very recently, a new type of charge qubit, called the charge quadrupole (CQ), has been proposed [20–22]. In the CQ qubit, an electron resides in a triple-quantum-dot system, giving rise to three electron states. In the lateral geometry, the tunneling between the two outermost dots are neglected, and one is left with only two barriers to address [20, 23]. It is argued that if the energies of the two barriers can be kept equal for the duration of the operation, and the same can be done for the energies of the two outmost dots, we are left with a decoherence free subspace against charge noise with which the fidelity may be substantially improved [20]. However, practically such a stringent requirement is difficult to satisfy, and even a slight deviation would cause considerable leakage as the leaked state is energetically very close to the qubit states. In order to suppress the leakage, composite pulses are proposed [21, 24].

In this Letter, we present a simple yet effective strategy to suppress the leakage thus protecting the decoherence free subspace. We propose that the triple dots can alternatively be fabricated in a triangle, in which the tunneling between the two outmost dots are amplified. This

tunnel coupling effectively separates the leaked state and qubit states, reducing leakage. We performed analytical and numerical analyses of the effect of the introduced tunnel coupling on the system, and found that the leakage can be suppressed by as much as five orders of magnitude. Further improvement of control fidelities is possible when composite pulses are applied to triangular triple quantum dots.

Model. A triple-quantum-dot system in triangular geometry is shown in Fig. 1, where the dots are labelled by 1, 2, 3, and the bending angle θ controls the shape of the triangle. When $\theta = 90^\circ$, the system is identical to the lateral triple dots considered in [20]. When only one electron is present in the system, we may define a set of “position basis” as $\{|100\rangle = c_1^\dagger|\text{vac}\rangle, |010\rangle =$

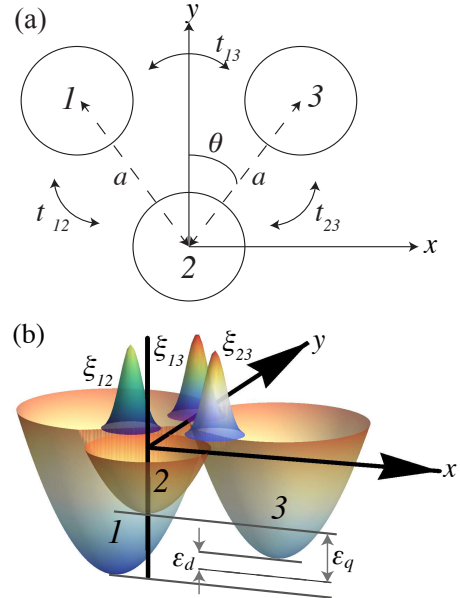


FIG. 1: (a) A schematic graph of the triangular triple dots viewing from $+z$ direction. (b) The confinement potential. ξ_{jk} is the barrier height between the j^{th} and k^{th} dot that is used in the Hund-Mulliken calculation. ϵ_q and ϵ_d are the quadrupolar and dipolar detuning energies respectively.

*Electronic address: x.wang@cityu.edu.hk

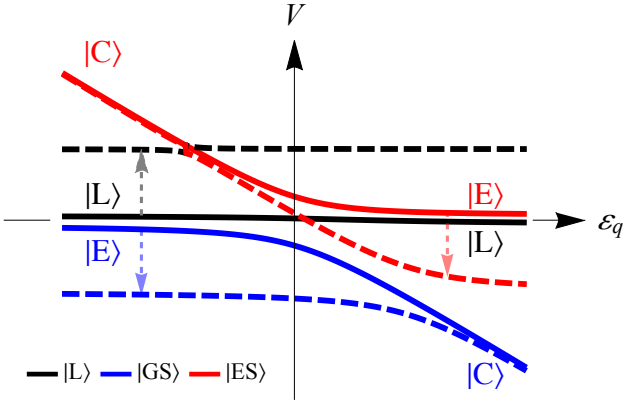


FIG. 2: Schematic figure of the energy spectrum of H_{CQ} [Eq. (2)] as a function of ε_q . The blue (red, black) solid line shows the eigenenergy of state $|GS\rangle$ ($|ES\rangle$, $|\tilde{L}\rangle$) when $|t_{13}| = 0$. The corresponding dashed lines show the levels when $t_{13} > 0$. The arrows indicate how the energies of the states are modified by t_{13} .

$c_2^\dagger|\text{vac}\rangle, |001\rangle = c_3^\dagger|\text{vac}\rangle\}$, where c_j^\dagger creates an electron on the j^{th} dot and $|\text{vac}\rangle$ is the vacuum state. Considering the fact that the electron can hop between any two dots, the Hamiltonian can be written as

$$\tilde{H}_{CQ} = \begin{pmatrix} \varepsilon_1 & -t_{12} & -t_{13} \\ -t_{12} & \varepsilon_2 & -t_{23} \\ -t_{13} & -t_{23} & \varepsilon_3 \end{pmatrix}, \quad (1)$$

where ε_j is the electron energy in the j^{th} dot and t_{jk} is the tunneling energy between the j^{th} and k^{th} dot. Comparing to the lateral-triple-dot case considered in [20], the additional terms involving t_{13} have significant effects on reduction of leakage as shall be demonstrated below.

The charge quadrupole (CQ) qubit is defined in the ‘‘even-odd’’ bases, $\{|C\rangle = |010\rangle, |E\rangle = (|100\rangle + |001\rangle)/\sqrt{2}, |L\rangle = (|100\rangle - |001\rangle)/\sqrt{2}\}$, where $|C\rangle$ and $|E\rangle$ are the logical bases, and $|L\rangle$ a leaked state. Under this set of bases, the Hamiltonian of a CQ qubit is

$$H_{CQ} = \begin{pmatrix} -\varepsilon_q & -t & 0 \\ -t & -t_{13} & 0 \\ 0 & 0 & t_{13} \end{pmatrix} + H_{\text{leak}}, \quad (2)$$

where

$$H_{\text{leak}} = \begin{pmatrix} 0 & 0 & \Delta t \\ 0 & 0 & \varepsilon_d \\ \Delta t & \varepsilon_d & 0 \end{pmatrix}, \quad (3)$$

$t = (t_{12} + t_{23})/\sqrt{2}$, $\Delta t = (t_{23} - t_{12})/\sqrt{2}$, $\varepsilon_d = (\varepsilon_1 - \varepsilon_3)/2$, and $\varepsilon_q = (\varepsilon_1 + \varepsilon_3)/2 - \varepsilon_2$ (an overall energy shift of $(\varepsilon_1 + \varepsilon_3)/2$ has been removed). When $\Delta t = \varepsilon_d = 0$, the leaked state has an energy of t_{13} and completely decouples from the qubit states. The CQ qubit is then operated by varying t and ε_q . Nevertheless, maintaining $\Delta t = \varepsilon_d = 0$ is a difficult practice. One must keep $t_{12} =$

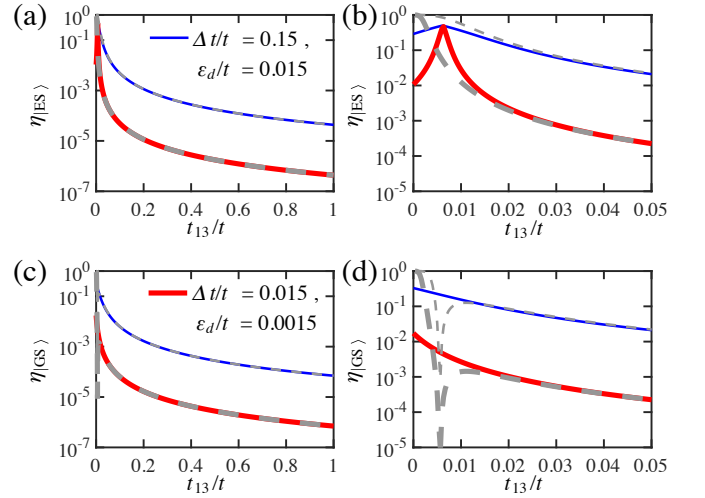


FIG. 3: Leakage as a function of tunneling rate t_{13} where $\Delta t > 0$ and $\varepsilon_d > 0$ for (a) $|ES\rangle$ at $\varepsilon_q = 800\mu\text{eV}$ and (c) $|GS\rangle$ at $\varepsilon_q = -800\mu\text{eV}$. $t = 10\mu\text{eV}$. Solid (dashed) line shows the numerical (analytical) solution. (b) ((d)) is a zoom-in version of the small ε_q range of (a) ((c)).

t_{23} and $\varepsilon_1 = \varepsilon_3$ for the duration of an operation, requiring extremely high precision in control, and a slight deviation from the equalities would cause leakage.

For the convenience of later discussions, we define leakage as follows. We denote the eigenstates of the noisy Hamiltonian [Eq. (2)] as $|GS\rangle, |ES\rangle$ and $|\tilde{L}\rangle$. $|GS\rangle$ and $|ES\rangle$ are the ground state and excited state respectively that are used to encode qubit states, while $|\tilde{L}\rangle$ is the leaked state with mostly $|L\rangle$ character. The former two states can be expressed as

$$\begin{aligned} |GS\rangle &= \alpha_{GS}|C\rangle + \beta_{GS}|E\rangle + \gamma_{GS}|L\rangle, \\ |ES\rangle &= \alpha_{ES}|C\rangle + \beta_{ES}|E\rangle + \gamma_{ES}|L\rangle. \end{aligned} \quad (4)$$

The leakage is then defined as the probability of $|L\rangle$ in $|GS\rangle$ or $|ES\rangle$, i.e. $\eta_{|GS\rangle} = |\gamma_{GS}|^2$, $\eta_{|ES\rangle} = |\gamma_{ES}|^2$.

Below, we shall demonstrate that increasing t_{13} moves the leaked state far away in energy and substantially reduces leakage.

Results. Figure 2 shows qualitatively the energy levels of the Hamiltonian H_{CQ} [Eq. (2)]. When $|\varepsilon_q| \gg 0$ (away from the avoided crossing), the eigenstates are predominantly $|C\rangle$, $|E\rangle$ or $|L\rangle$ states, respectively. Also in this range, the energy of the state which is mainly $|E\rangle$ character becomes asymptotically close to that of $|L\rangle$, causing heavy leakage when Δt or ε_d are nonzero. To further understand how t_{13} changes leakage, we have performed analytical calculations on Eq. (2) treating H_{leak} as a perturbation, and details can be found in the Supplemental Material [25]. We have shown that the energy difference between $|GS\rangle$ and $|\tilde{L}\rangle$ (denoted as ΔE_{GS}), and that between $|ES\rangle$ and $|\tilde{L}\rangle$ (ΔE_{ES}) can be expressed in the limit

of $|\varepsilon_q| \gg 0$ as [25]:

$$\begin{aligned} \Delta E_{GS} &= E_{GS} - E_L \approx -2t_{13} - \delta, & (\varepsilon_q < 0) \\ \Delta E_{ES} &= E_{ES} - E_L \approx -2t_{13} + \delta, & (\varepsilon_q > 0) \end{aligned} \quad (5)$$

where $\delta = t^2/|\varepsilon_q - t_{13}|$ is typically small when $t < t_{13} \ll |\varepsilon_q|$. Therefore, the introduction of t_{13} does two things: it moves the energy of the $|E\rangle$ state down by $-t_{13}$ (away from the avoided crossing), while moving the energy of the $|L\rangle$ state up by t_{13} , causing an energy difference of $2t_{13}$ between them. The larger t_{13} is, the further apart the two states are, and the smaller the leakage would be. This effect is shown as the dashed lines in Fig. 2 where the arrows indicate the effect of t_{13} .

Figure 3 compares the numerical and perturbation theory calculations of the leakage as a function of t_{13}/t when both Δt and ε_d are non-zero. The numerical solutions (shown as solid lines) are derived from a direct diagonalization of Eq. (2), while the perturbation theory results are from Sec. I of the Supplemental Material [25]. From Fig. 3(a) and (c) we see that increasing t_{13} indeed reduces leakage drastically. When t_{13} is about 20% of t , the leakage can be reduced by roughly three orders of magnitude for the case with $\Delta t/t = 0.15$ and $\varepsilon_d/t = 0.015$, and five orders of magnitude for the case with $\Delta t/t = 0.015$ and $\varepsilon_d/t = 0.0015$. When the magnitude of t_{13} is approaching t (which is experimentally feasible when the three dots form an equilateral triangle as shall be discussed later), the reduction of leakage is more than three orders of magnitude for the case with larger Δt and ε_d , and about five orders of magnitude for the case with smaller Δt and ε_d .

It is also interesting to note the existence of a cusp at $t_{13}/t \approx 0.006$ in Fig. 3(b), a zoomed-in version of Fig. 3(a). This happens because when $t_{13} = 0$, $|ES\rangle$ is slightly above $|L\rangle$ in energy. When t_{13} is increased to $t_{13}/t \approx 0.006$ at these parameters, $|ES\rangle$ first moves down closer to $|L\rangle$, and then moves further away from $|L\rangle$ as t_{13} is further increased. Therefore the leakage first increases, then decreases substantially. Since the increase of leakage only happens for very small t_{13} , we believe that it does not affect our main results. We also note that at this very point the non-degenerate perturbation theory would fail, thus the disagreement between analytical and numerical results in Fig. 3(b) and (d) [26].

We note that Δt and ε_d do not contribute equally to the leakage. The leakage can be approximately shown to depend quadratically on both $\Delta t/t_{13}$ and ε_d/t_{13} with different prefactors [25]. For a more detailed discussion as well as results of leakage when only one of Δt and ε_d is allowed to be nonzero, see [25]. In any case, the leakage to $|L\rangle$ is substantially reduced when t_{13} is increased.

We further investigate how t_{13} can be increased by simply altering the geometry of the triple dots. This information is not in the model Hamiltonian Eq. (1), and we must calculate using a microscopic theory. In this work, we calculate various parameters in Eq. (1) using standard Hund-Mulliken approximation, which retains the lowest energy level in each dot. The details of the calculation

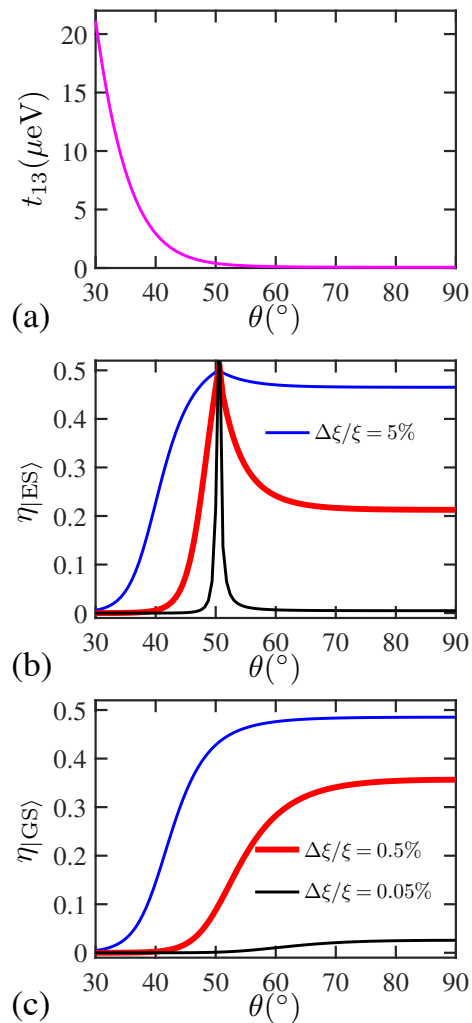


FIG. 4: (a) t_{13} as a function of bending angle θ for $\varepsilon_q = 800\mu\text{eV}$. (b), (c): Leakage as a function of bending angle θ due to $\Delta\xi$ for (b) $|ES\rangle$ at $\varepsilon_q = 800\mu\text{eV}$ and (c) $|GS\rangle$ at $\varepsilon_q = -800\mu\text{eV}$. Blue (red, black) line shows result for $\Delta\xi/\xi = 5\%$, (0.5%, 0.05%), which corresponds to $\Delta t/t = 21\%$, (2.1%, 0.21%) and $\varepsilon_d/t = 1.3$, (13%, 0.13%) in the language of Eq. (2). The parameters are $a = 150\text{nm}$, $\hbar\omega_0 = 0.7\text{meV}$, $\xi = 2.2\text{meV}$, $\xi_{13} = 0$, $m^* = 0.067m_e$ for GaAs.

can be found in [25]. While ε_d can be tuned in the calculation by simply changing the dot energies, Δt is varied, in the microscopic calculations, by altering the heights of the tunneling barriers between dots, ξ_{12} , ξ_{23} and ξ_{13} as indicated in Fig. 1(b). Nevertheless, our calculations reveal that differences between ξ_{12} and ξ_{23} , which we denote as $\Delta\xi = (\xi_{12} - \xi_{23})/2$, will indirectly give rise to dipolar detuning noise ε_d . We therefore will not separate Δt noise but instead use $\Delta\xi$ in the relevant discussions. We also define $\xi = (\xi_{12} + \xi_{23})/2$ for convenience.

Figure 4(a) shows the magnitude of t_{13} as a function of the bending angle θ (cf. Fig. 1). For $60^\circ < \theta < 90^\circ$, t_{13} is negligibly small but then increases rapidly when $\theta < 60^\circ$. We also note that $\theta < 30^\circ$ is unphysical due to the fact that dot 1 and dot 3 start to overlap substantially and our

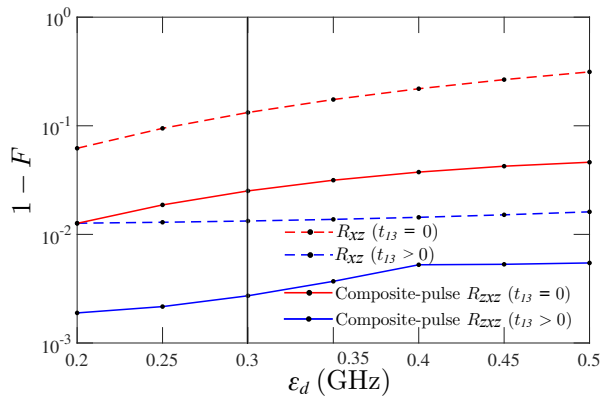


FIG. 5: Infidelities of $R_{\hat{x}+\hat{y}}(\frac{\pi}{2})$ as functions of ε_d for linear (red/upper two lines, $t_{13} = 0$) and triangular triple-quantum dot (blue/lower two lines, $t_{13} > 0$). Black-filled circles are the maximally minimized infidelity for numerically optimized pulses corresponding to the given ε_d . The vertical black solid line indicates a typical value of ε_d that is consistent with recent experiments [27]. Two types of pulse sequences are compared, the naive two-step rotation, $R_{\hat{z}}(\varphi)R_{\hat{x}}(\zeta)$ (dashed lines), and the leakage suppressing composite-pulse, $R_{\hat{z}}(\varphi)R_{\hat{x}}(\zeta)R_{\hat{z}}(\varphi)$ (solid lines).

triple-dot model is no longer valid. Therefore the results are not shown in that range. Fig. 4(b) and (c) show the leakage η as functions of the bending angle θ for different levels of $\Delta\xi/\xi$. Since t_{13} increases as θ is reduced, these figures are best viewed from right to left. Fig. 4(b) shows the leakage for the excited state. For the range of $60^\circ \lesssim \theta \lesssim 90^\circ$ the leakage remains mostly constant, which is consistent with the results shown in Fig. 4(a) that t_{13} is almost zero. As θ approaches about 50° , the leakage increases because t_{13} is increased to a small positive value which brings the excited and the leaked state very close in energy, also consistent with the observation in Fig. 3(b). After that as θ is reduced below 50° , t_{13} rapidly increases and the leakage is drastically suppressed. Overall, we see that for lateral triple dots ($\theta = 90^\circ$) the leakage can be as large as 0.47 for $\Delta\xi/\xi = 5\%$, but it can be suppressed by 80% when $\theta \approx 37^\circ$, and further down to a very small value ($\approx 3 \times 10^{-6}$) when θ approaches 30° . Fig. 4(c) shows the leakage of the ground state as a function of θ . The leakage monotonically decreases as θ is decreased from 90° to 30° because a positive t_{13} brings the ground state further away from the leaked state without crossing it, as is clear from Fig. 2. It is again obvious that when $\theta \lesssim 50^\circ$ the reduction of leakage is substantial.

From Fig. 4(b) and (c), it is also remarkable that for $\Delta\xi/\xi = 0.5\%$ the level of leakage far exceeds that of $\Delta t/t = 0.15$ shown in Fig. 3. This is due to the fact that $\Delta\xi$ not only gives rise to Δt but also ε_d , which for this particular case is $\varepsilon_d/t = 0.13$, a very large value. As is shown in [25], ε_d contributes more than Δt with a much larger prefactor, therefore the leakage in this case

is very large. To complete the discussion, we have also performed calculations where ε_d is varied and $\Delta\xi$ is kept at 0 (note that t_{12} and t_{23} values are still affected), and the results are shown in [25].

An alternative strategy to suppress leakage is the use of composite pulses with appropriately chosen parameters [21]. We compare the method to ours and also study the benefit when we combine the two methods, i.e. implementing composite pulses with a nonzero t_{13} . We briefly review the key points of the composite pulse method in [25], together with details of our implementation. We take the rotation of $\pi/2$ around axis $\hat{x} + \hat{y}$, $R_{\hat{x}+\hat{y}}(\pi/2)$, as an example. This operation can either be achieved by a two-piece pulse-sequence, $R_{xz}(\varphi, \zeta) = R_{\hat{z}}(\varphi)R_{\hat{x}}(\zeta)$, if no correction to noises is desired, or a z - x - z sequence $R_{zxx}(\varphi, \zeta) = R_{\hat{z}}(\varphi)R_{\hat{x}}(\zeta)R_{\hat{z}}(-\varphi)$, which can correct noises with appropriately chosen parameters [21, 25]. We have also considered a finite rise time of 50 ps for every pulse in implementation [25]. Fig. 5 shows the infidelity of different implementations of $R_{\hat{x}+\hat{y}}(\pi/2)$. The dashed lines show results of the naive R_{xz} sequence, while solid lines the R_{zxx} composite pulse sequence. Red (upper two) lines are results with $t_{13} = 0$, and $t_{13} = 7.5$ GHz ($\approx 30 \mu\text{eV}$) for blue (lower two) lines. We see that while the composite pulse sequences indeed reduce the leakage and consequently improves the infidelity, a nonzero t_{13} is more effective: the results from the R_{xz} sequence with $t_{13} = 7.5$ GHz has lower error than results from R_{zxx} sequence with $t_{13} = 0$ for the range of ε_d considered. Nevertheless, the combination of the two methods, i.e. using composite pulse sequence while keeping $t_{13} > 0$, yields the lowest error, which is of the order of 10^{-3} .

Conclusions. We suggest a simple yet effective strategy for protecting the computational subspace of a CQ qubit implemented in a triple-quantum-dot device, i.e by fabricating triple quantum dots in a triangle. The introduced t_{13} as a consequence of the triangular architecture can lift the energy separation of two energetically close states ($|L\rangle$ and $|E\rangle$) thus substantially reduces the leakage. Microscopic calculation reveals that leakage reduction becomes evident when the bending angle $\theta \lesssim 50^\circ$, and when $\theta = 30^\circ$ (i.e. the three dots forming an equilateral triangle), the leakage is suppressed by several orders of magnitude compared to those in a lateral array as originally conceived. Our results should help in achieving precise control of a CQ qubit, a promising candidate to realize quantum information processing in semiconductor quantum devices.

Acknowledgements. This work is supported by the Research Grants Council of the Hong Kong Special Administrative Region, China (Grant Nos. CityU 21300116, CityU 11303617), the National Natural Science Foundation of China (Grant Nos. 11604277, 11874312), and the Guangdong Innovative and Entrepreneurial Research Team Program (Grant No. 2016ZT06D348).

-
- [1] T. Hayashi, T. Fujisawa, H. D. Cheong, Y. H. Jeong, and Y. Hirayama, *Phys. Rev. Lett.* **91**, 226804 (2003).
- [2] T. Fujisawa, T. Hayashi, H. Cheong, Y. Jeong, and Y. Hirayama, *Physica E* **21**, 1046 (2004).
- [3] T. Fujisawa, T. Hayashi, and S. Sasaki, *Rep. Prog. Phys.* **69**, 759 (2006).
- [4] G. Shinkai, T. Hayashi, T. Ota, and T. Fujisawa, *Phys. Rev. Lett.* **103**, 056802 (2009).
- [5] H.-O. Li, G. Cao, G.-D. Yu, M. Xiao, G.-C. Guo, H.-W. Jiang, and G.-P. Guo, *Nat. Commun.* **6**, 7681 (2015).
- [6] D. R. Ward, D. Kim, D. E. Savage, M. G. Lagally, R. H. Foote, M. Friesen, S. N. Coppersmith, and M. A. Eriksson, *npj Quantum Inf.* **2**, 16032 (2016).
- [7] J. Gorman, D. G. Hasko, and D. A. Williams, *Phys. Rev. Lett.* **95**, 090502 (2005).
- [8] K. D. Petersson, J. R. Petta, H. Lu, and A. C. Gossard, *Phys. Rev. Lett.* **105**, 246804 (2010).
- [9] Y. Dovzhenko, J. Stehlik, K. D. Petersson, J. R. Petta, H. Lu, and A. C. Gossard, *Phys. Rev. B* **84**, 161302 (2011).
- [10] Z. Shi, C. B. Simmons, D. R. Ward, J. R. Prance, R. T. Mohr, T. S. Koh, J. K. Gamble, X. Wu, D. E. Savage, M. G. Lagally, M. Friesen, S. N. Coppersmith, and M. A. Eriksson, *Phys. Rev. B* **88**, 075416 (2013).
- [11] Z. V. Penfold-Fitch, F. Sfigakis, and M. R. Buitelaar, *Phys. Rev. Applied* **7**, 054017 (2017).
- [12] B.-C. Wang, B.-B. Chen, G. Cao, H.-O. Li, M. Xiao, and G.-P. Guo, *EPL* **117**, 57006 (2017).
- [13] G. Cao, H.-O. Li, T. Tu, L. Wang, C. Zhou, M. Xiao, G.-C. Guo, H.-W. Jiang, and G.-P. Guo, *Nat. Commun.* **4**, 1401 (2013).
- [14] D. Kim, D. Ward, C. Simmons, J. K. Gamble, R. Blume-Kohout, E. Nielsen, D. Savage, M. Lagally, M. Friesen, S. Coppersmith, *et al.*, *Nat. Nanotechnol.* **10**, 243 (2015).
- [15] G. Cao, H.-O. Li, G.-D. Yu, B.-C. Wang, B.-B. Chen, X.-X. Song, M. Xiao, G.-C. Guo, H.-W. Jiang, X. Hu, and G.-P. Guo, *Phys. Rev. Lett.* **116**, 086801 (2016).
- [16] C. H. Wong, *Phys. Rev. B* **93**, 035409 (2016).
- [17] M. Serina, C. Kloeffer, and D. Loss, *Phys. Rev. B* **95**, 245422 (2017).
- [18] Y.-C. Yang, S. N. Coppersmith, and M. Friesen, *Phys. Rev. A* **95**, 062321 (2017).
- [19] B.-C. Wang, G. Cao, H.-O. Li, M. Xiao, G.-C. Guo, X. Hu, H.-W. Jiang, and G.-P. Guo, *Phys. Rev. Applied* **8**, 064035 (2017).
- [20] M. Friesen, J. Ghosh, M. A. Eriksson, and S. N. Coppersmith, *Nat. Commun.* **8**, 15923 (2017).
- [21] J. Ghosh, S. Coppersmith, and M. Friesen, *Physical Review B* **95**, 241307 (2017).
- [22] V. Kornich, M. G. Vavilov, M. Friesen, and S. Coppersmith, *New J. Phys.* **20**, 103048 (2018).
- [23] X.-C. Yang, G. X. Chan, and X. Wang, *Phys. Rev. A* **98**, 032334 (2018).
- [24] Y. Sun, J. Zhang, and L.-A. Wu, *e-print arXiv:1712.05442* (2017).
- [25] See Supplemental Material at [URL will be inserted by publisher] for details.
- [26] Since this disagreement happens for a very small t_{13} and as t_{13} is further increased, the leakage is substantially reduced as desired, we will not perform a calculation with degenerate perturbation theory to resolve the disagreement, as that is unimportant for our main results.
- [27] X. Mi, J. V. Cady, D. M. Zajac, J. Stehlik, L. F. Edge, and J. R. Petta, *Appl. Phys. Lett.* **110**, 043502 (2017).

Supplementary material

In this Supplemental Material we provide necessary details complementary to results shown in the main text.

I. CALCULATION OF LEAKAGE FROM PERTURBATION THEORY

In this section we calculate the leakage from non-degenerate perturbation theory. As discussed in the main text, leakage is caused either by $\varepsilon_d \neq 0$ or $\Delta t \neq 0$. When $\varepsilon_d = \Delta t = 0$, the eigenvalues of the Hamiltonian H_{CQ} [Eq. (2) in the main text] are

$$E_{GS} = \frac{1}{2} \left[-(\varepsilon_q + t_{13}) - |\varepsilon_q - t_{13}| \sqrt{1 + \alpha^2} \right], \quad (\text{S-1a})$$

$$E_{ES} = \frac{1}{2} \left[-(\varepsilon_q + t_{13}) + |\varepsilon_q - t_{13}| \sqrt{1 + \alpha^2} \right], \quad (\text{S-1b})$$

$$E_L = t_{13}, \quad (\text{S-1c})$$

and its eigenvectors (written in $\{|C\rangle, |E\rangle, |L\rangle\}$ basis) are

$$|GS\rangle^{(0)} = \left(\frac{\beta + \gamma}{\chi\sqrt{\alpha^2 + (1 + \beta\gamma)^2}}, \frac{|\alpha|}{\sqrt{\alpha^2 + (1 + \beta\gamma)^2}}, 0 \right), \quad (\text{S-2a})$$

$$|ES\rangle^{(0)} = \left(\frac{\beta - \gamma}{\chi\sqrt{\alpha^2 + (1 - \beta\gamma)^2}}, \frac{|\alpha|}{\sqrt{\alpha^2 + (1 - \beta\gamma)^2}}, 0 \right), \quad (\text{S-2b})$$

$$|L\rangle^{(0)} = (0, 0, 1), \quad (\text{S-2c})$$

where $\alpha = |2t/(\varepsilon_q - t_{13})|$, $\beta = \text{sgn}(\varepsilon_q - t_{13})$, $\chi = \text{sgn}(t)$ and $\gamma = \sqrt{1 + \alpha^2}$. We have kept χ to cover the case in which t may become negative, although in our work t is always positive ($\chi = 1$). The superscript (0) indicates that these are zeroth order results.

Either a nonzero ε_d or Δt causes leakage. We calculate their effects on the leakage using non-degenerate perturbation theory. Therefore, the analytical results shown below are valid when ε_d and Δt are small, while $|t_{13}|$ is reasonably large such that the eigenstates are non-degenerate.

Perturbation theory suggests that the leakage is inversely proportional to the distance in energy between the two states concerned, i.e. $\eta_{|GS\rangle} \propto 1/(E_{GS} - E_L)$, and $\eta_{|ES\rangle} \propto 1/(E_{ES} - E_L)$. We have

$$\begin{aligned} \Delta E_{GS} &= E_{GS} - E_L \\ &= \frac{1}{2} \left\{ -(\varepsilon_q + t_{13}) - \left[-(\varepsilon_q - t_{13}) \sqrt{1 + \alpha^2} \right] \right\} - t_{13} \quad (\varepsilon_q < 0) \\ &\approx \frac{1}{2} \left[-\varepsilon_q - t_{13} + (\varepsilon_q - t_{13}) \left(1 + \frac{\alpha^2}{2} \right) \right] - t_{13} \\ &= -2t_{13} - \delta, \end{aligned} \quad (\text{S-3})$$

and

$$\begin{aligned} \Delta E_{ES} &= E_{ES} - E_L \\ &= \frac{1}{2} \left\{ -(\varepsilon_q + t_{13}) + \left[(\varepsilon_q - t_{13}) \sqrt{1 + \alpha^2} \right] \right\} - t_{13} \quad (\varepsilon_q > 0) \\ &\approx \frac{1}{2} \left[-\varepsilon_q - t_{13} + (\varepsilon_q - t_{13}) \left(1 + \frac{\alpha^2}{2} \right) \right] - t_{13} \\ &= -2t_{13} + \delta, \end{aligned} \quad (\text{S-4})$$

where $\delta = t^2/|\varepsilon_q - t_{13}|$. These are Eq. (5) in the main text. The approximation is made under the assumption that $|\varepsilon_q| \gg t_{13}$ and $|\varepsilon_q| \gg t$, which is valid as the leakage becomes more prominent in large $|\varepsilon_q|$ regime.

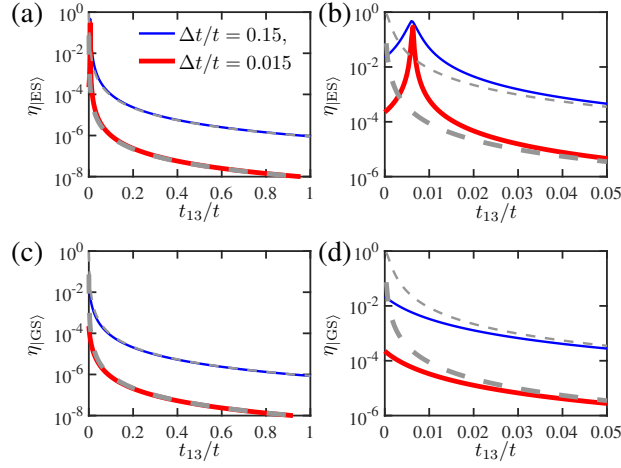
To the first order perturbation correction, the eigenstates are (up to $\mathcal{O}[\alpha^3]$):

$$\begin{aligned} |GS\rangle^{(1)} &= |GS\rangle^{(0)} + \Delta t |GS\rangle_{\Delta t}^{(1)} + \varepsilon_d |GS\rangle_{\varepsilon_d}^{(1)} \\ &= \frac{1}{c} \left(\frac{1}{2\chi} \alpha - \frac{3}{16\chi} \alpha^3, 1 - \frac{1}{8} \alpha^2, - \left\{ \left[\frac{\chi}{4t_{13}} \alpha + \frac{(\varepsilon_q - 4t_{13})\chi}{32t_{13}^2} \alpha^3 \right] \Delta t + \left[\frac{1}{2t_{13}} + \frac{\varepsilon_q - 2t_{13}}{16t_{13}^2} \alpha^2 \right] \varepsilon_d \right\} \right), \end{aligned} \quad (\text{S-5a})$$

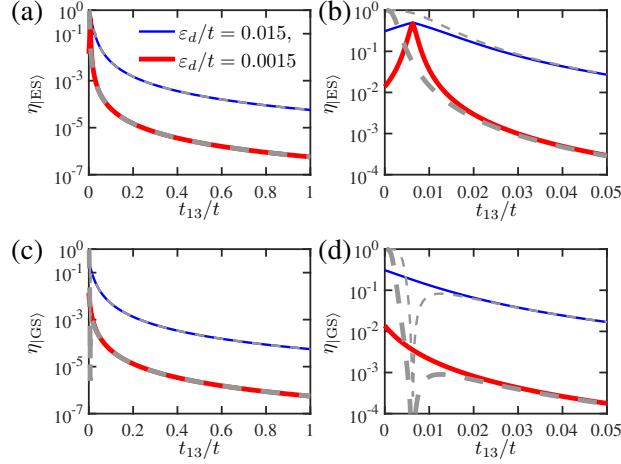
$$\begin{aligned} |ES\rangle^{(1)} &= |ES\rangle^{(0)} + \Delta t |ES\rangle_{\Delta t}^{(1)} + \varepsilon_d |ES\rangle_{\varepsilon_d}^{(1)} \\ &= \frac{1}{c} \left(-\frac{1}{2\chi} \alpha + \frac{3}{16\chi} \alpha^3, 1 - \frac{\alpha^2}{8}, \left[\frac{\chi}{4t_{13}} \alpha + \frac{(\varepsilon_q - 4t_{13})\chi}{32t_{13}^2} \alpha^3 \right] \Delta t - \left[\frac{1}{2t_{13}} + \frac{\varepsilon_q - 2t_{13}}{16t_{13}^2} \right] \varepsilon_d \right), \end{aligned} \quad (\text{S-5b})$$

where c is the normalization constant, and the subscript Δt (ε_d) indicates correction arising from Δt (ε_d). We note that since the leakage is only based on the coefficient of $|L\rangle$, for which the second order correction is zero, our discussion of leakage is in fact valid to the second order of Δt and ε_d .

Severe leakage happens when $|\varepsilon_q| \gg 0$. If $\varepsilon_q \rightarrow +\infty$, leakage happens between $|ES\rangle$ and $|L\rangle$, and we denote $\eta \approx \eta_{|ES\rangle} = |\langle L|ES\rangle|^2$. If $\varepsilon_q \rightarrow -\infty$, leakage happens between $|GS\rangle$ and $|L\rangle$, $\eta \approx \eta_{|GS\rangle} = |\langle L|GS\rangle|^2$. These results are plotted, with comparison to numerical results, in Fig. 3 in the main text as well as in Fig. S1 and Fig. S2. Fig. 3 in the main text shows the case in which both Δt and ε_d are nonzero. For completeness, we show the results of the case with $\Delta t \neq 0$ and $\varepsilon_d = 0$ in Supplementary Fig. S1, and those of the case with $\Delta t = 0$ and $\varepsilon_d \neq 0$ in Supplementary



Supplementary Figure S1: Leakage as a function of tunneling rate t_{13} where $|\Delta t| > 0$ for (a) $|ES\rangle$ at $\varepsilon_q = 800\mu\text{eV}$ and (c) $|GS\rangle$ at $\varepsilon_q = -800\mu\text{eV}$. The parameters are $t = 10\mu\text{eV}$, $\varepsilon_d = 0$. Solid (dashed) line shows the numerical (analytical) solution. (b) ((d)) is a zoomed-in version of the small ε_q range of (a) ((c)).



Supplementary Figure S2: Leakage as a function of tunneling rate t_{13} where $|\varepsilon_d| > 0$ for (a) $|ES\rangle$ at $\varepsilon_q = 800\mu\text{eV}$ and (c) $|GS\rangle$ at $\varepsilon_q = -800\mu\text{eV}$. The parameters are $t = -10\mu\text{eV}$ and $\Delta t = 0$. Solid (dashed) line shows the numerical (analytical) solution. (b) ((d)) is a zoomed-in version of the small ε_q range of (a) ((c)).

Fig. S2. Overall the behavior seen from Supplementary Figs. S1 and S2 are very similar to that of Fig. 3 in the main text, i.e. t_{13} substantially reduces leakage, except that for $|ES\rangle$ the leakage first increases at very small t_{13} values (because it is brought closer to $|L\rangle$) and then decreases as $|ES\rangle$ moves further away.

It is interesting to further simplify the expression of the leakage by discarding the terms of $\mathcal{O}[\alpha]^3$ or higher order (since $\alpha = \left| \frac{2t}{\varepsilon_q - t_{13}} \right| \rightarrow 0$ when $|\varepsilon_q| \gg |t_{13}|$), the leakage probabilities can be approximated by

$$\eta \approx \eta_{GS}^{(2)} = \eta_{ES}^{(2)} = \left[\frac{\alpha \chi \left(\frac{\Delta t}{2t_{13}} \right)}{\sqrt{4 + \frac{\alpha^4}{16} + \alpha^2 \left(\frac{\Delta t}{2t_{13}} \right)^2}} - \frac{\left(\frac{\varepsilon_d}{t_{13}} \right)}{\sqrt{4 + \frac{\alpha^4}{16} + \left(\frac{\varepsilon_d}{t_{13}} \right)^2}} \right]^2 \quad \text{when } |\varepsilon_q| \gg t_{13}, \quad (\text{S-6})$$

where the superscript (2) indicates that the results is valid up to the second order in the perturbation theory. Further

expanding α terms in the denominators and keep only up to $\mathcal{O}[\alpha]^2$, we have a simplified expression of leakage

$$\eta = \eta_{\Delta t} + \eta_{\varepsilon_d} \approx \left(\frac{\alpha}{4}\right)^2 \left(\frac{\Delta t}{t_{13}}\right)^2 + \frac{1}{2} \left(\frac{\varepsilon_d}{t_{13}}\right)^2. \quad (\text{S-7a})$$

$$\frac{\eta_{\varepsilon_d}}{\eta_{\Delta t}} \approx \frac{\frac{1}{2} \left(\frac{\varepsilon_d}{t_{13}}\right)^2}{\left(\frac{\alpha}{4}\right)^2 \left(\frac{\Delta t}{t_{13}}\right)^2} = \frac{8\varepsilon_d^2}{\alpha^2 \Delta t^2} \quad (\text{S-7b})$$

This expression indicates that both Δt and ε_d contribute to the leakage quadratically; however the coefficient in front of ε_d is much larger than Δt , indicating that for similar levels of ε_d and Δt , the former causes much more severe leakage. This also explains why in Supplementary Figs. S1 and S2 the leakage levels in both cases are comparable while Δt is about 10 times ε_d .

II. DETAILS OF HUND-MULLIKEN CALCULATION

The Hamiltonian of a triple-quantum-dot system (in position basis) is

$$H = \sum_{j=1}^3 h(\mathbf{r}_j) \quad (\text{S-8})$$

where $h(\mathbf{r}_j)$ is the single-particle Hamiltonian of particle j

$$h(\mathbf{r}_j) = \frac{1}{2m^*} (\mathbf{p}_j - e\mathbf{A}_j)^2 + V(\mathbf{r}_j) \quad (\text{S-9})$$

Since there is only one electron, two-particle interactions are absent. There are three possible states (denoted as position basis $\{|100\rangle, |010\rangle, |001\rangle\}$ in the main text).

Figure 1 of the main text shows the confinement potential the electron experiences in a triple-quantum-dot device. The positions of the dots are defined as

$$\mathbf{R}_1 = (-a \sin \theta, a \cos \theta), \quad (\text{S-10a})$$

$$\mathbf{R}_2 = (0, 0), \quad (\text{S-10b})$$

$$\mathbf{R}_3 = (a \sin \theta, a \cos \theta), \quad (\text{S-10c})$$

where a is the interdot distance and θ is the bending angle. The confinement potential is defined as a sum of two parts,

$$V(x, y) = V_0(x, y) + G(x, y). \quad (\text{S-11})$$

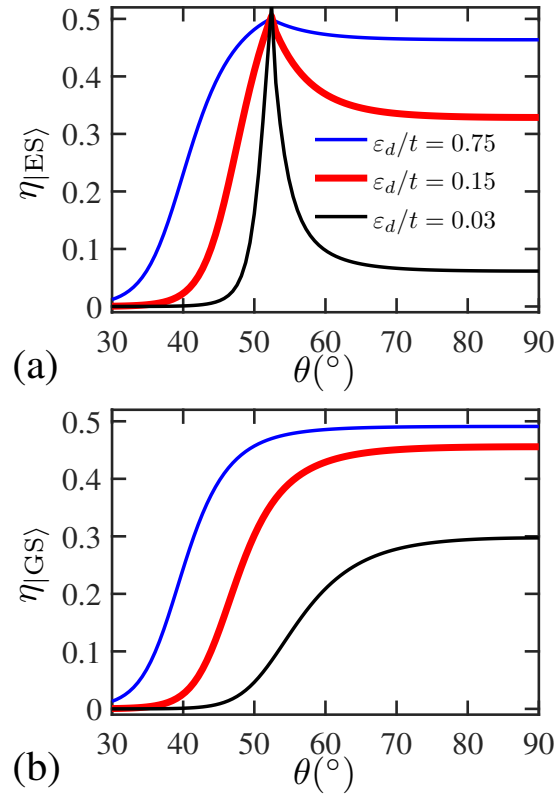
The first part, $V_0(x, y)$, has a conventional quadratic form and is divided into three regions in x-y plane, each of which corresponds to a quantum dot,

$$V(x, y) = \begin{cases} v_2 & \text{if } x > 0 \text{ and } y < -x \tan \theta + \frac{a}{2 \cos \theta}, \\ v_3 & \text{if } x > 0 \text{ and } y > -x \tan \theta + \frac{a}{2 \cos \theta}, \\ v_2 & \text{if } x < 0 \text{ and } y < x \tan \theta + \frac{a}{2 \cos \theta}, \\ v_1 & \text{if } x < 0 \text{ and } y > x \tan \theta + \frac{a}{2 \cos \theta}, \end{cases} \quad (\text{S-12})$$

where

$$v_j = \frac{1}{2} m^* \omega_0^2 |\mathbf{r} - \mathbf{R}_j|^2 + \mu_j. \quad (\text{S-13})$$

The second part, $G(x, y)$, encapsulates information of the tunable barriers (ξ_{jk}) between adjacent dots in triangular



Supplementary Figure S3: Leakage arises from dipole detuning noise $|\varepsilon_d|$ as a function of bending angle θ for (a) $|ES\rangle$ where $\varepsilon_q = 800\mu\text{eV}$ and (b) $|GS\rangle$ where $\varepsilon_q = -0.8\mu\text{eV}$. The parameters are $a = 150\text{nm}$, $\hbar\omega_0 = 0.7\text{meV}$, $\xi = 2.2\text{meV}$, $\xi_{13} = 0\text{meV}$, $m^* = 0.017m_e$ for GaAs.

form of the triple dots ($\xi_{13} = 0$ when the geometry of triple dots is close to lateral form),

$$G(x, y) = \sum_{j < k}^3 G_{jk}(x, y, \mathbf{R}_{jk}, \xi_{jk}), \quad (\text{S-14})$$

where

$$G_{jk} = \xi_{jk} \exp \left[-\frac{32|\mathbf{r}_{jk} - \mathbf{R}_{jk}|^2}{a^2} \right], \quad (\text{S-15a})$$

$$\mathbf{R}_{12} = \left(-\frac{a}{2} \sin \theta, \frac{a}{2} \cos \theta \right), \quad (\text{S-15b})$$

$$\mathbf{R}_{23} = \left(\frac{a}{2} \sin \theta, \frac{a}{2} \cos \theta \right) \quad (\text{S-15c})$$

$$\mathbf{R}_{13} = (0, a \cos \theta) \quad (\text{S-15d})$$

With the confinement potential defined, we can solve the Hamiltonian by adopting the Hund-Mulliken approximation which keeps only the lowest Fock-Darwin state. The ground state is approximated to be the solution of a harmonic oscillator

$$\psi_j(\mathbf{r}) = \frac{1}{a_B \sqrt{\pi}} \exp \left[-\frac{1}{2a_B^2} |\mathbf{r} - \mathbf{R}_j|^2 \right], \quad (\text{S-16})$$

where $a_B = \sqrt{\hbar/(m^*\omega_0)}$ and $j = 1, 2, 3$ refers to the three quantum dots. The approximated single particle wave function is then obtained by orthonormalizing the three Fock-Darwin states by the following transformation

$$\{\psi_1, \psi_2, \psi_3\}^\top = \mathcal{O}^{1/2} \{\Psi_1, \Psi_2, \Psi_3\}^\top \quad (\text{S-17})$$

where \mathcal{O} is the overlap matrix defined to be $\mathcal{O}_{jk} = \langle \psi_i | \psi_j \rangle$. The matrix elements in the Hamiltonian, Eq. (1) in the main text, can then be determined by

$$\varepsilon_j = \langle \Psi_j | h(\mathbf{r}_j) | \Psi_j \rangle, \quad (\text{S-18a})$$

$$t_{jk} = -\langle \Psi_j | h(\mathbf{r}_j) | \Psi_k \rangle. \quad (\text{S-18b})$$

Diagonalization of the Hamiltonian yields the eigenvalues and eigenstates for a particular set of dot parameters.

In Fig. 4 of the main text we have shown the case for which $\Delta\xi$, the relative height of barriers, is varied. As noted in the main text, due to the nature of the microscopic calculation, $\Delta\xi$ not only changes Δt but also indirectly ε_d . In order to complete the discussion, we show the case for which ε_d is varied in the microscopic calculation (of course Δt is at the same time indirectly changed) in Supplementary Fig. S3. The main message is similar to that from Fig. 4 of the main text: For $|ES\rangle$, as θ reduces to about 50° the leakage first increases but then drops drastically. For $|GS\rangle$ the leakage reduces monotonically as θ is reduced from 60° to 30° . Overall, having the triple quantum dots in an equilateral triangle (therefore a nonzero t_{13}) reduces the leakage substantially.

III. SUPPRESSION OF LEAKAGE USING PULSE SEQUENCE

Leakage can be alternatively suppressed using pulse sequences as proposed in [21]. Here we perform a comparison between the effectiveness of pulse sequences and our method, and we also study the benefit when we combine the two.

Using the language of [21], our Hamiltonian becomes a combination of three terms (up to an overall energy shift of $\varepsilon_q/2 + t_{13}/2$):

$$H_z(\varepsilon_q) = - \begin{pmatrix} \frac{\varepsilon_q - t_{13}}{2} & 0 & 0 \\ 0 & -\frac{\varepsilon_q - t_{13}}{2} & 0 \\ 0 & 0 & 0 \end{pmatrix}, \quad H_x(t) = - \begin{pmatrix} 0 & t & 0 \\ t & 0 & 0 \\ 0 & 0 & 0 \end{pmatrix}, \quad H_{\text{leak}}(\varepsilon_d) = - \begin{pmatrix} 0 & 0 & 0 \\ 0 & 0 & \varepsilon_d \\ 0 & \varepsilon_d & -\frac{\varepsilon_q + 3t_{13}}{2} \end{pmatrix}. \quad (\text{S-19})$$

Compared to [21], our Hamiltonian has an extra minus sign, but this would not affect the results.

Reference [21] only considered noises arising from $\delta\varepsilon_d$. We denote a rotation of angle ϕ around axis \hat{r} as $R_{\hat{r}}(\phi)$, and the rotations around \hat{z} and \hat{x} in a noisy $\delta\varepsilon_d$ environment are

$$R_{\hat{z}}(\varphi) = U_z(\varepsilon_q, \varepsilon_d, \varphi) = e^{-i[H_z(\varepsilon_q) + H_{\text{leak}}(\varepsilon_d)]\varphi/(2\varepsilon_q)}, \quad (\text{S-20a})$$

$$R_{\hat{x}}(\zeta) = U_x(t, \varepsilon_d, \zeta) = e^{-i[H_x(t) + H_{\text{leak}}(\varepsilon_d)]\zeta/(2t)}. \quad (\text{S-20b})$$

An arbitrary single-qubit rotation about an axis in xy plane can therefore be decomposed into elementary rotations $R_{\hat{z}}(\varphi)$ and $R_{\hat{x}}(\zeta)$. For example, we define a “ z - x - z ” sequence as

$$\begin{aligned} R_{\text{zxx}}(\varphi, \zeta) &= R_{\hat{z}}(\varphi)R_{\hat{x}}(\zeta)R_{\hat{z}}(-\varphi) \\ &= U_z(\varepsilon_q, \varepsilon_d, \varphi)U_x(t, \varepsilon_d, \zeta)U_z(-\varepsilon_q, \varepsilon_d, \varphi). \end{aligned} \quad (\text{S-21})$$

It has been found that when

$$\varepsilon_q = -\frac{t\varphi}{4} \cot\left(\frac{\zeta}{4}\right), \quad (\text{S-22})$$

The first order contribution arising from ε_d vanishes in the “bang-bang” limit (i.e. the pulses rise/set instantaneously to the desired values) [21]. If the pulses have a finite (nonzero) rising time, Eq. (S-22) substantially reduces the first order contribution from ε_d but not completely. One then needs to numerically adjust the height and duration of individual pulses in order to optimize the suppression of leakage.

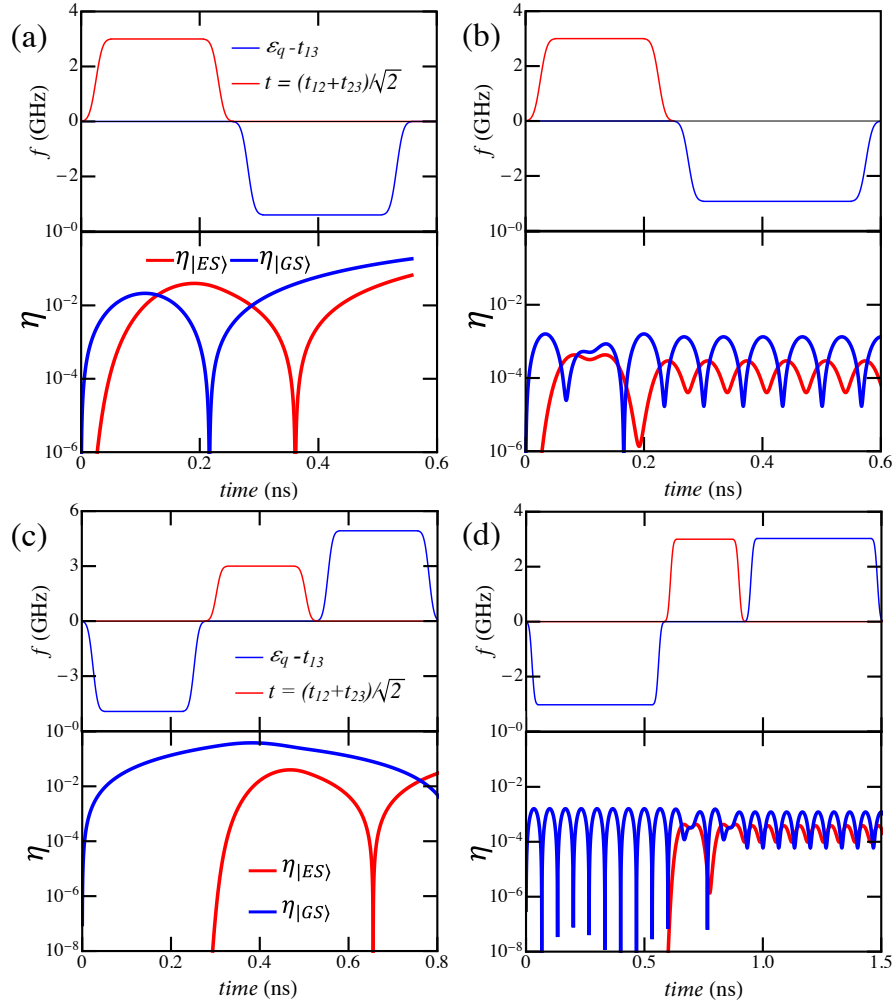
As an example, we study the rotation $R_{\hat{x}+\hat{y}}(\pi/2)$ that can be decomposed as

$$R_{\hat{x}+\hat{y}}(\pi/2) = e^{-7i\pi/8} R_{\text{zx}}(-7\pi/4, \pi/2) = e^{-7i\pi/8} R_{\hat{z}}(-7\pi/4)R_{\hat{x}}(\pi/2), \quad (\text{S-23})$$

if no correction is desired. Nevertheless, a “ z - x - z ” sequence must be employed if we want to suppress the leakage:

$$R_{\hat{x}+\hat{y}}(\pi/2) = R_{\text{zxx}}(\pi/4, \pi/2) = R_{\hat{z}}(\pi/4)R_{\hat{x}}(\pi/2)R_{\hat{z}}(-\pi/4). \quad (\text{S-24})$$

We consider two cases: $t_{13} = 0$ and $t_{13} = 7.5 \text{ GHz} \approx 30 \text{ } \mu\text{eV}$ with t fixed at 3 GHz. We also take into account the



Supplementary Figure S4: Numerically optimized gate operation for $R_{\hat{x}+\hat{y}}(\pi/2)$ at $\epsilon_d = 0.3$ GHz. (a), (b): The pulse sequence and leakage probabilities for naive two-pulse sequence, $R_{xz}(\varphi, \zeta) = R_{\hat{x}}(\varphi)R_{\hat{z}}(\zeta)$. (c), (d): The pulse sequence and leakage probabilities for z - x - z sequence (with noise correction), $R_{zxx}(\varphi, \zeta) = R_{\hat{z}}(\varphi)R_{\hat{x}}(\zeta)R_{\hat{z}}(\varphi)$. (a), (c): $t_{13} = 0$. (b), (d): $t_{13} = 7.5$ GHz. In each panel, the top subfigure shows the pulse sequence with f denoting the pulse amplitude, and the bottom subfigure shows the leakage probabilities.

finite rise time of 50 ps for every pulse [21]. Numerical optimization is performed with respect to the fidelity defined as

$$F = \frac{1}{12} \left[\text{Tr}(\mathcal{U}\mathcal{U}^\dagger) + \left| \text{Tr}(U_{\text{target}}^\dagger \mathcal{U}) \right|^2 \right], \quad (\text{S-25})$$

where U_{target} is the desired operation, and \mathcal{U} the actual evolution. Leakage probabilities η are defined as $\eta_{|GS\rangle} = |\langle L|\mathcal{U}(t; t=0)|GS\rangle_{t=0}|^2$ where $|GS\rangle_{t=0} = |E\rangle$, and $\eta_{|ES\rangle} = |\langle L|\mathcal{U}(t; t=0)|ES\rangle_{t=0}|^2$ where $|ES\rangle_{t=0} = |C\rangle$.

Numerical results are shown in Fig. S4. It can be observed that for the naive pulse sequences (R_{xz}), the leakage simply accumulates throughout the gate operation, ending up with a large leakage at the conclusion of the sequence. [Fig. S4(a)]. When the composite pulses are employed, the leakage first accumulates but then decreases, and the leakage for the gate is smaller compared to the previous case [Fig. S4(c)]. In both cases, applying a nonzero t_{13} reduces the leakage substantially. For naive sequences the results shown in Fig. S4(b) have a leakage level two orders of magnitude lower than that of Fig. S4(a). For corrected composite sequences, the nonzero t_{13} reduces the leakage by about one order of magnitude [compare Fig. S4(d) and Fig. S4(c)].